



Study on open charm hadron production and angular correlation in high-energy nuclear collisions

Hai Wang¹ · Jin-Hui Chen¹

Received: 25 September 2020 / Revised: 29 October 2020 / Accepted: 21 November 2020 / Published online: 19 January 2021
© China Science Publishing & Media Ltd. (Science Press), Shanghai Institute of Applied Physics, the Chinese Academy of Sciences, Chinese Nuclear Society 2021

Abstract We study the production and angular correlation of charm hadrons in hot and dense matter produced in high-energy nuclear–nuclear collisions within a multiphase transport model (AMPT). By triggering additional charm–anticharm quark pair production in the AMPT, the model describes the D^0 nuclear modification factor in the low and intermediate p_T regions in Au + Au collisions at $\sqrt{s_{NN}} = 200$ GeV reasonably well. Further exploration of the D^0 pair azimuthal angular correlation for different centralities shows clear evolution from low-multiplicity to high-multiplicity events, which is associated with the number of charm quark interactions with medium partons during AMPT transport.

Keywords Heavy-ion collision · Heavy flavor · Nuclear modification factor · Two-particle correlations

1 Introduction

In high-energy nuclear collisions, heavy-flavor quarks are produced predominantly in the initial phase because of their large mass ($m_{c/b} > \Lambda_{\text{QCD}}$). The modification of

their production in transverse momentum (p_T) due to energy loss and radial flow and in azimuth due to anisotropic flows is sensitive to the heavy quark dynamics in the hot and dense strongly interacting quark–gluon plasma (QGP) [1–3]. Recent experimental measurements of high- p_T D-meson production at RHIC and LHC energies show strong suppression of central heavy-ion collisions [4–6], suggesting significant energy loss by charm quarks inside the QGP medium.

There is a great deal of interest in the use of heavy-flavor quarks to constrain the transport properties of the QGP [7, 8]. During their propagation through the QGP, heavy-flavor quarks interact with the constituents of the medium and lose some of their momentum and thus can reveal some of the QGP properties. However, the mechanism of the in-medium modification of heavy quarks is not fully understood [9]. A theoretical study of charm production has found that the cross section of gluons makes a large contribution, where heavy flavor appears from gluon splitting only in the late stages of the parton shower evolution [10]. We have studied the collisional energy loss term by adding an additional $c\bar{c}$ pair production in a multiphase transport model (AMPT), which significantly improves the description of the charm hadron p_T spectrum and elliptic flow in Au + Au collisions at $\sqrt{s_{NN}} = 200$ GeV [11]. Here, we extend the previous study and focus on the collision centrality dependence of D-meson production, the nuclear modification factor, and the azimuthal angular correlation.

Analysis of multiparticle angular correlations is a powerful tool for exploring the properties of the QGP and the underlying mechanism of particle production in hot quantum chromodynamic (QCD) matter [12–20]. Unlike light quarks and gluons, heavy quarks suppress small-angle

This work was supported in part by the Strategic Priority Research Program of the Chinese Academy of Sciences (No. XDB34030200) and the National Natural Science Foundation of China (Nos. 12025501, 11890710, and 11775288).

✉ Jin-Hui Chen
chenjinhui@fudan.edu.cn

¹ Key Laboratory of Nuclear Physics and Ion-beam Application (MOE), Fudan University, Shanghai 200433, China

gluon radiation, which results in a small radiated energy loss [21, 22]. In hadron–hadron collisions, which are dominated by the initial production effect, a distinct feature appears in the azimuthal angular correlation of $D\bar{D}$, with clear suppression on the near side and enhancement on the away side [23]. In nuclear–nuclear collisions, the angular correlation may be affected by the interactions of charm quarks in the QGP, which is argued to be a signature of a strongly coupled QGP owing to the collective partonic wind effect [23]. The evolution of the azimuthal angular correlation of charm hadron pairs in the QGP has not been carefully studied in a realistic transport calculation, and that lack motivates the current work.

2 Charm quark production in AMPT model

The AMPT model is a hybrid model [24]. It has been extensively used for studying the bulk medium using the microscopic dynamical processes of evolving systems, as reported in recent papers [25–27]. In this model, the initial conditions are taken from the HIJING event generator [28, 29]. In the default AMPT model, the partonic matter consists only of minijet partons from HIJING. It is different in the string melting scenario, in which the hadrons generated by HIJING are dissociated according to their valence quark structures, and the resulting partonic matter is thus much denser. The evolution of the partonic matter is simulated using the parton cascade model ZPC [30], and the partons are converted to hadrons after they stop scattering. In the default AMPT model, the partons are first combined with their parent strings, which then fragment using the Lund string fragmentation model [31]. In the string melting AMPT model, the nearest partons are converted into hadrons via the coalescence model [24]. In both versions of the AMPT model, the scattering of hadrons is described by a relativistic transport model [32].

The initial production of charm quarks in the AMPT model is handled by the HIJING model. It includes pair production ($q + \bar{q} \rightarrow Q + \bar{Q}$, $g + g \rightarrow Q + \bar{Q}$) and gluon splitting ($g \rightarrow Q + \bar{Q}$). The gluon splitting process is implemented using a parton shower method similar to that in a general Monte Carlo event generator [31]. The pair production cross section in perturbative QCD at the leading order can be expressed as

$$\frac{d\sigma^{c\bar{c}}}{dp_T^2 dy_1 dy_2} = K \sum_{a,b} x_1 f_a(x_1, p_T^2) x_2 f_b(x_2, p_T^2) \frac{d\sigma^{ab \rightarrow c\bar{c}}}{d\hat{t}}. \quad (1)$$

Here, y_1 and y_2 are the rapidities of the produced charm quarks, respectively. Further, x_1 and x_2 are the fractions of momentum carried by the initial partons; the relationship between them is $x_1 = x_T(e^{y_1} + e^{y_2})/2$,

$x_2 = x_T(e^{-y_1} + e^{-y_2})$, where $x_T = 2p_T/\sqrt{s}$. K is a factor that accounts for higher-order corrections of the charm quark production and typically has a value of $K \approx 2$ [29]. In addition, $f(x, p_T^2)$ are the default parton distribution functions in HIJING, which are taken to be the Duke–Owens structure function set 1 [33].

From Eq. (1), one can obtain the total inclusive cross section $\sigma^{c\bar{c}}$ by integration at a low p_T cutoff p_0 :

$$\sigma^{c\bar{c}} = \int_{p_0^2}^{s/4} dp_T^2 dy_1 dy_2 \frac{1}{2} \frac{d\sigma^{c\bar{c}}}{dp_T^2 dy_1 dy_2}. \quad (2)$$

For a nucleon–nucleon collision, the average number of semihard parton collisions at impact parameter b is $\sigma^{c\bar{c}} T_N(b)$, where $T_N(b)$ is the partonic overlap function between the two nucleons at impact parameter b [28]. The probability of multiple charm pair production is given by

$$g_j(b) = \frac{[\sigma^{c\bar{c}} T_N(b)]^j}{j!} e^{-\sigma^{c\bar{c}} T_N(b)}, \quad (3)$$

with $j \geq 1$. The HIJING model has two components with two key parameters, the minijet transverse momentum cutoff p_0 and the soft interaction cross section σ_{soft} . σ_{soft} controls the elastic, inelastic, and total cross sections. The production probability for soft interactions without hard processes is

$$g_0(b) \left[1 - e^{-\sigma_{\text{soft}} T_N(b)} \right] e^{-\sigma^{c\bar{c}} T_N(b)}. \quad (4)$$

The elastic, inelastic, and total cross sections of binary collisions are thus calculated in the model [28, 29].

Because the differential cross section of charm quark production is smaller than that of light quarks, we trigger charm production using a specific p_T threshold in the normal AMPT event to increase the simulation efficiency. This is done by adding the trigger parameters to the AMPT code to call the related subroutine, where $\text{IHPR2}(3) = 3$ is used to trigger heavy quark hard scattering, $\text{IHPR2}(18) = 0$ is used for charm production, and $\text{HIPR1}(10)$ is used for the trigger p_T threshold [29]. The trigger will then change the probability of charm quark production and thus the entire event structure [28]. In particular, if we select a large p_T^{trig} value (i.e., 20 GeV/c), such rare processes with large p_T scattering occur most frequently when the impact parameter of the collisions is small, and thus, the partonic overlap is large. At a small impact parameter, the production of the charm quark pair is enhanced. The probability of charm quark pair production in the triggered event is

$$g_j^{\text{trig}}(b) = \frac{[\sigma^{c\bar{c}}(p_0)T_N(b)]^j}{j!} \left\{ 1 - \left[\frac{\sigma^{c\bar{c}}(p_0) - \sigma^{c\bar{c}}(p_T^{\text{trig}})}{\sigma^{c\bar{c}}(p_0)} \right]^j \right\} e^{-\sigma^{c\bar{c}}(p_0)T_N(b)}. \quad (5)$$

From the above equation, when $p_T^{\text{trig}} = p_0$, $g_j^{\text{trig}}(b)$ is consistent with $g_j(b)$ in Eq. (3). Summing over $j \geq 1$ leads to the expected total probability of having at least one charm quark pair with $p_T \geq p_T^{\text{trig}}$:

$$g^{\text{trig}}(b) = 1 - e^{-\sigma^{c\bar{c}}(p_T^{\text{trig}})T_N(b)}. \quad (6)$$

Because $g_j^{\text{trig}}(b)$ differs from $g_j(b)$, the triggering of charm quark pair production changes the production rate of other particles in the same event [28]. This trigger algorithm was initially implemented in HIJING to study rare processes such as high-momentum jets [28, 29], and it is extended to study charm quark production and transport dynamics in the hot QCD medium [11].

In this study, the default and string melting AMPT models (version v2.26t5) are used, where additional high- p_T (20 GeV/ c) charm quark pair triggers are implemented to improve the simulation efficiency. In both AMPT models, the event statistics are 2×10^5 , 2×10^6 , and 1×10^6 for inclusive Au + Au and pp collisions at $\sqrt{s_{\text{NN}}} = 200\text{GeV}$ and p -Pb collisions at $\sqrt{s_{\text{NN}}} = 5.02\text{TeV}$, respectively. A few key input parameters of the program, including the parton cascade cross section, $\sigma_p = 3\text{mb}$, and the Lund string fragmentation function, $a = 0.55$, $b = 0.15\text{GeV}^{-2}$, are applied [25]. For details on the other parameters, readers are referred to the program manual [24].

3 Results and discussion

3.1 D^0 meson p_T distribution and R_{AA} in AMPT model

Figure 1 presents the D^0 meson p_T spectrum in 0–10% central Au + Au collisions at $\sqrt{s_{\text{NN}}} = 200\text{GeV}$ and compares them with the AMPT model calculations. One sees that the AMPT model predicts only $\sim 1/4$ of the D^0 yield for the centrality analyzed. Ref. [34] reports that when an extended version of the AMPT model is obtained by removing the p_0 cutoff for the heavy quark production cross section, their inclusion in the total minijet cross section will improve the description of the charm production significantly. We learned that the procedure implemented in Ref. [34] is similar to the approach applied in

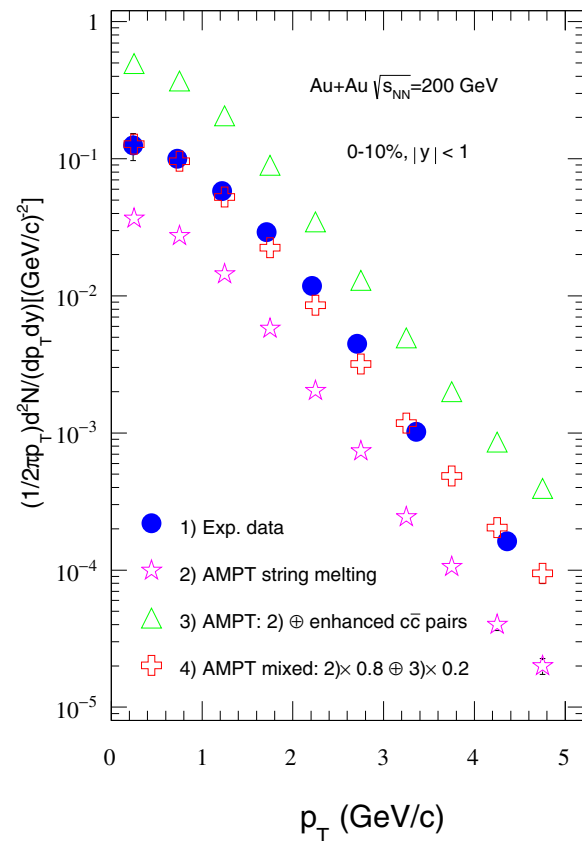


Fig. 1 (Color online) D^0 meson p_T spectra in central Au + Au collisions at $\sqrt{s_{\text{NN}}} = 200\text{GeV}$. Open symbols represent results of AMPT model calculation for different configurations; solid symbols are experimental data [4]

our earlier study [11]. Because the extended version developed in Ref. [34] is not publicly accessible yet, we further explore the study using our approach. The green open triangles in Fig. 1 show the D^0 p_T spectrum in the AMPT model with an additional charm–anticharm quark trigger. It overpredicts the data. Because the slopes of the two AMPT calculations in Fig. 1 are the same, one can build a new event sample to describe the data with a fraction determined by the data. The red crosses in Fig. 1 represent the results in such a new event sample, with 80% of the normal AMPT distribution (pink open stars) plus 20% of the AMPT with an additional trigger on charm quark pair production (green triangles). We refer to the new sample as the AMPT mixed sample and use it to study the charm production and evolution in the hot and dense QCD matter in the following.

Using the above p_T distributions, we investigate the nuclear modification factor R_{AA} of the D^0 meson in central Au + Au collisions at $\sqrt{s_{\text{NN}}} = 200\text{GeV}$, because R_{AA} is well established as a sensitive observable for the study of

the interaction of hard partons with the medium. It is usually defined as

$$R_{AA}(p_T) = \frac{1}{N_{\text{coll}}} \frac{d^2 N_{AA}/(dp_T dy)}{d^2 N_{pp}/(dp_T dy)}, \quad (7)$$

where N_{coll} represents the number of binary collisions in the reaction.

Figure 2 compares the results of our calculations with experimental data. The typical calculations for pp collisions using the default or string melting AMPT model both exhibit enhancement at a p_T value of approximately 1.5 GeV/c and strong suppression at intermediate p_T , although their magnitudes are much larger than those of the experimental data. This result, in combination with the normal AMPT distribution presented in Fig. 1, suggests that charm production in pp collisions at $\sqrt{s} = 200$ GeV is greatly underpredicted by the AMPT model compared to that in Au + Au collisions. This behavior is also observed by studying the collision energy dependence of the total cross sections of charm–anticharm quark pairs [34]. We thus build the new event sample of pp collisions following the procedure used for Au + Au collisions with the same percentages of normal and triggered AMPT events. The new R_{AA} describes the experimental data well.

In the AMPT model, the interaction between charm quarks and the medium is simulated by parton elastic scattering. It has been noted that the elastic collisional energy loss is dominant for heavy flavors below a moderately high p_T , for example, for the charm hadron at $p_T \leq 5 - 6$ GeV/c in Au + Au collisions at $\sqrt{s_{NN}} = 200$ GeV/c [35]. Therefore, it is understood that the AMPT model with only collisional energy loss and no radiative energy loss can describe the R_{AA} data at low and intermediate p_T . In the parton cascade of the AMPT model, the parton cross section and its angular distribution

determine the strength of the interaction between heavy quarks and the expanding medium [11, 34]. The follow-up hadronic interactions are mainly for light-flavor hadrons. For heavy-flavor hadrons, we consider only the decays with large mass resonances [24].

3.2 D^0 meson azimuthal angular correlation

We use the two-particle azimuthal angular correlation function to study the charm quark dynamics evolution in the hot and dense medium using the AMPT model, in which multi-parton scattering may have a significant effect on the correlation function $C(\Delta\phi)$. In our study, $C(\Delta\phi)$ is built as follows:

$$C(\Delta\eta, \Delta\phi) = \frac{S(\Delta\eta, \Delta\phi)/N_{\text{pairs}}^{\text{signal}}}{B(\Delta\eta, \Delta\phi)/N_{\text{pairs}}^{\text{mixed}}}, \quad (8)$$

where $\Delta\eta$ is the relative pseudorapidity, and $\Delta\phi$ is the relative azimuthal angle between charm hadron pairs. The signal pair distribution, $S(\Delta\eta, \Delta\phi)$, represents the yield of charm hadron pairs that come from the same event:

$$S(\Delta\eta, \Delta\phi) = \frac{d^2 N_{\text{pairs}}^{\text{signal}}}{d\Delta\eta d\Delta\phi}. \quad (9)$$

In addition, $B(\Delta\eta, \Delta\phi)$ is built from the mixed event charm hadron pairs distribution:

$$B(\Delta\eta, \Delta\phi) = \frac{d^2 N_{\text{pairs}}^{\text{mixed}}}{d\Delta\eta d\Delta\phi}, \quad (10)$$

which is flat in our calculation.

The one-dimensional correlation function along $\Delta\phi$ can be constructed from the $C(\Delta\eta, \Delta\phi)$ distribution by integrating over $\Delta\eta$:

$$C(\Delta\phi) = A \times \frac{\int S(\Delta\eta, \Delta\phi) d\Delta\eta}{\int B(\Delta\eta, \Delta\phi) d\Delta\eta}, \quad (11)$$

where the normalization constant A is estimated from $N_{\text{pairs}}^{\text{mixed}}/N_{\text{pairs}}^{\text{signal}}$, which depends on the details of the mixed event process. For example, the current event is mixed with eight other events in the same collision centrality interval to improve the statistical power of the background estimation. The two-dimensional (2D) charm hadron correlation function as a function of $\Delta\eta$ and $\Delta\phi$ is analyzed in different centrality classes of Au + Au collisions at $\sqrt{s_{NN}} = 200$ GeV and high-multiplicity p -Pb collisions at $\sqrt{s_{NN}} = 5.02$ TeV with $0.3 < p_T < 5$ GeV/c for trigger particles and associated particles of interest.

Figure 3 presents the centrality dependence of the D^0 meson azimuthal angular correlations in the default and string melting AMPT models, where the former represents a combination of initial production plus the multi-parton

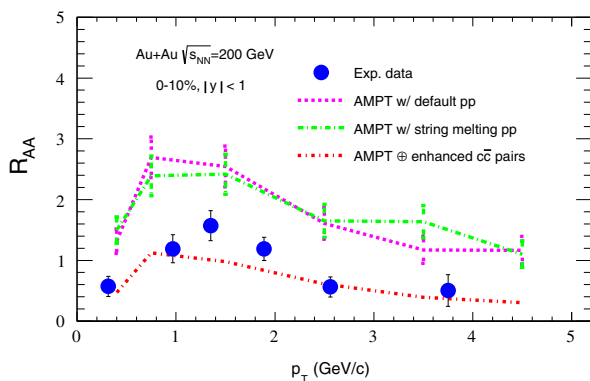


Fig. 2 (Color online) D^0 meson R_{AA} in central Au + Au collisions at $\sqrt{s_{NN}} = 200$ GeV. Dashed lines represent results of AMPT model calculation for different configurations. Data points are experimental measurements [4]

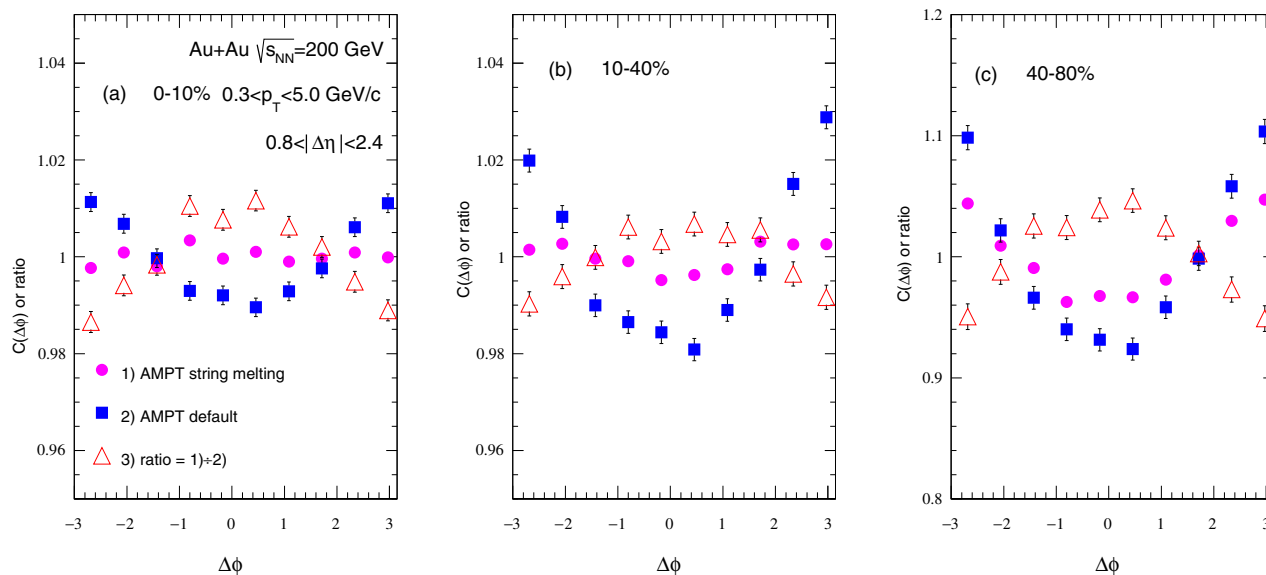


Fig. 3 D^0 meson azimuthal angular correlations vs. centrality in Au + Au collisions at $\sqrt{s_{NN}} = 200$ GeV for default or string melting AMPT models and various ratios of the two

scattering effect, and the latter is dominated by the initial production effect. The open charm hadron azimuthal angular correlations in the default AMPT model show clear suppression at $|\Delta\phi| \approx 0$ and enhancement at $|\Delta\phi| \approx \pi$. This is expected from the initial back-to-back charm–anticharm quark pair production due to their large mass and momentum. However, the distribution in the string melting AMPT model differs from that in the default AMPT model. In peripheral Au + Au collisions, finite parton scatterings smear the angular correlation with a similar concave distribution versus $|\Delta\phi|$. In central Au + Au collisions, strong parton scatterings affect the correlation with a flat or near convex distribution. If the dynamics of parton cascade is traced by counting the number of collisions of charm quark with other partons, the value in central collisions could be 5–6 times higher than that in peripheral collisions [11]. The multi-parton scatterings reshape the charm hadron angular correlations. The evolution of the shape of the correlation function associated with the number of parton collisions suggests that the charm hadron azimuthal angular correlations may be an experimental observable that can be used to quantitatively measure the charm hadron interaction with the medium. Comparisons of future measurements using upgrades of existing experiments or new experiments with current calculations will elucidate the charm quark dynamics in hot and dense media.

To eliminate the trigger effect in the initial stage and focus on the multi-parton scattering effect, we define the ratio of the correlation functions of the default and string melting AMPT models:

$$\text{ratio} = \frac{C(\Delta\phi)_{\text{melting}}}{C(\Delta\phi)_{\text{default}}}. \quad (12)$$

The results are shown as open triangles in Fig. 3. They show a convex distribution versus $\Delta\phi$ owing to the multi-parton scattering interaction in the string melting AMPT model. The result for peripheral collisions is far from the flat distribution among the three centralities, probably because charm quarks usually lose the most energy in the first collision [11].

As noted in [23], the strong collective flow of pp or Pb–Pb collisions at LHC energies will significantly modify the charm hadron azimuthal correlation. We performed the transport calculation in this study. Figure 4 shows the open charm hadron azimuthal angular correlation function $C(\Delta\phi)$ in high-multiplicity p -Pb collisions at $\sqrt{s_{NN}} = 5.02$ TeV, where the multiplicity is calculated using the charged particle pseudorapidity distributions within $|\eta| < 0.5$ [25]. The result in the default AMPT model is similar to the distribution of peripheral Au + Au collisions at $\sqrt{s_{NN}} = 200$ GeV, whereas the string melting AMPT model shows a distribution closer to that of central Au + Au collisions at $\sqrt{s_{NN}} = 200$ GeV. The ratio of the string melting and default AMPT models shows a clear convex distribution. These results, together with the elliptic flow study of p -Pb collisions from the AMPT model in comparison with data [17], confirm that strong partonic collectivity affects the charm hadron pair azimuthal angular correlation.

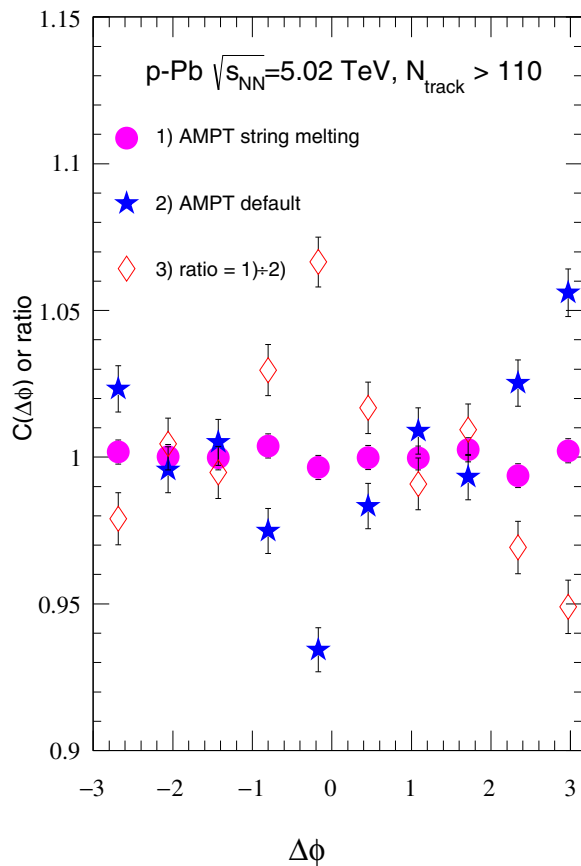


Fig. 4 D^0 azimuthal angular correlation function $C(\Delta\phi)$ in p -Pb collisions at $\sqrt{s_{NN}} = 5.02$ TeV within the multiplicity range $N_{\text{track}} > 110$ of AMPT model calculations

4 Summary and outlook

In summary, we studied the dynamic evolution of the charm hadron in the AMPT model with additional charm quark pair production. The model describes the D^0 meson nuclear modification factor in central Au + Au collisions at $\sqrt{s_{NN}} = 200$ GeV up to $p_T = 6$ GeV/ c . The results suggest that collisional energy loss is dominant for the D^0 meson in the low and intermediate p_T regions. The D^0 meson pair azimuthal angular correlations are studied for different centralities and from Au + Au collisions at $\sqrt{s_{NN}} = 200$ GeV to high-multiplicity p -Pb collisions at $\sqrt{s_{NN}} = 5.02$ TeV. The AMPT model shows clear smearing of the away-side charm hadron pair azimuthal angular correlation induced by parton scattering. Our study provides a method of quantitative study of the heavy-flavor dynamics in the hot and dense QGP created in high-energy nuclear collisions. It is also useful for future experiments with upgraded detectors at LHC-ALICE or for new experiments such as the RHIC-sPHENIX.

Acknowledgements We are grateful to Dr. Chen Zhong, who maintains the high-performance computer center at which the calculations for the current study were performed. We thank Dr. Song Zhang for discussions of the correlation function analysis.

Author contributions All authors contributed to the study conception and design. Material preparation, data collection and analysis were performed by Hai Wang and Jin-Hui Chen. The first draft of the manuscript was written by Hai Wang, and all authors commented on previous versions of the manuscript. All authors read and approved the final manuscript.

References

1. Z.B. Tang, W.M. Zha, Y.F. Zhang, An experimental review of open heavy flavor and quarkonium production at RHIC. Nucl. Sci. Tech. **31**, 81 (2020). <https://doi.org/10.1007/s41365-020-00785-8>
2. X. Luo, S. Shi, N. Xu et al., A study of the properties of the QCD phase diagram in high-energy nuclear collisions. Particles **3**, 278–307 (2020). <https://doi.org/10.3390/particles3020022>
3. X. Dong, Y.J. Lee, R. Rapp, Open heavy-flavor production in heavy-ion collisions. Annu. Rev. Nucl. Part. Sci. **69**, 417–445 (2019). <https://doi.org/10.1146/annurev-nucl-101918-023806>
4. L. Adamczyk, J.K. Adkins, G. Agakishiev et al., Observation of D^0 meson nuclear modifications in Au + Au collisions at $\sqrt{s_{NN}} = 200$ GeV. Phys. Rev. Lett. **113**, 142301 (2014). <https://doi.org/10.1103/PhysRevLett.113.142301>
5. J. Adam, D. Adamova, M.M. Aggarwal et al., Transverse momentum dependence of d-meson production in pb-pb collisions at $\sqrt{s_{NN}} = 2.76$ TeV. J. High Energy Phys. **03**, 081 (2016). [https://doi.org/10.1007/jhep03\(2016\)081](https://doi.org/10.1007/jhep03(2016)081)
6. A. Sirunyan, A. Tumasyan, W. Adam et al., Nuclear modification factor of d_0 mesons in pPb collisions at $\sqrt{s_{NN}} = 5.02$ TeV. Phys. Lett. B **782**, 474–496 (2018). <https://doi.org/10.1016/j.physletb.2018.05.074>
7. M. He, R. Rapp, Hadronization and charm-hadron ratios in heavy-ion collisions. Phys. Rev. Lett. **124**, 042301 (2020). <https://doi.org/10.1103/PhysRevLett.124.042301>
8. S. Cao, G. Coci, S.K. Das et al., Toward the determination of heavy-quark transport coefficients in quark-gluon plasma. Phys. Rev. C **99**, 054907 (2019). <https://doi.org/10.1103/PhysRevC.99.054907>
9. A. Andronic, F. Arleo, R. Arnaldi et al., Heavy-flavour and quarkonium production in the LHC era: from proton-proton to heavy-ion collisions. Eur. Phys. J. C **76**, 107 (2016). <https://doi.org/10.1140/epjc/s10052-015-3819-5>
10. Y.L. Dokshitzer, D. Kharzeev, Heavy quark colorimetry of QCD matter. Phys. Lett. B **519**, 199–206 (2001). [https://doi.org/10.1016/S0370-2693\(01\)01130-3](https://doi.org/10.1016/S0370-2693(01)01130-3)
11. H. Wang, J.H. Chen, Y.G. Ma et al., Charm hadron azimuthal angular correlations in Au + Au collisions at $\sqrt{s_{NN}} = 200$ GeV from parton scatterings. Nucl. Sci. Tech. **30**, 185 (2019). <https://doi.org/10.1007/s41365-019-0706-z>
12. G. Aad, B. Abbott, J. Abdallah et al., Observation of associated near-side and away-side long-range correlations in $\sqrt{s_{NN}} = 5.02$ TeV Proton-Lead Collisions with the ATLAS Detector. Phys. Rev. Lett. **110**, 182302 (2013). <https://doi.org/10.1103/PhysRevLett.110.182302>
13. S. Chatrchyan, V. Khachatryan, A.M. Sirunyan et al., Multiplicity and transverse momentum dependence of two- and four-particle correlations in pPb and PbPb collisions. Phys. Lett. B **724**, 213–240 (2013). <https://doi.org/10.1016/j.physletb.2013.06.028>

14. S. Acharya, D. Adamová, J. Adolphsson et al., Azimuthal anisotropy of heavy-flavor decay electrons in p-Pb collisions at $\sqrt{s_{NN}}=5.02$ TeV. *Phys. Rev. Lett.* **122**, 072301 (2019). <https://doi.org/10.1103/PhysRevLett.122.072301>
15. J. Adam, L. Adamczyk, J. Adams et al., Azimuthal harmonics in small and large collision systems at rhic top energies. *Phys. Rev. Lett.* **122**, 172301 (2019). <https://doi.org/10.1103/PhysRevLett.122.172301>
16. A. Adare, S. Afanasiev, C. Aidala et al., Measurement of two-particle correlations with respect to second-and third-order event planes in Au + Au collisions at $\sqrt{s_{NN}} = 200$ GeV. *Phys. Rev. C* **99**, 054903 (2019). <https://doi.org/10.1103/PhysRevC.99.054903>
17. A. Bzdak, G.L. Ma, Elliptic and triangular flow in p-pb and peripheral pb-pb collisions from parton scatterings. *Phys. Rev. Lett.* **113**, 252301 (2014). <https://doi.org/10.1103/PhysRevLett.113.252301>
18. J. Chen, D. Keane, Y.G. Ma et al., Antinuclei in heavy-ion collisions. *Phys. Rep.* **760**, 1–39 (2018). <https://doi.org/10.1016/j.physrep.2018.07.002>
19. L.Y. Zhang, J.H. Chen, Z.W. Lin et al., Two-particle angular correlations in heavy ion collisions from a multiphase transport model. *Phys. Rev. C* **99**, 054904 (2019). <https://doi.org/10.1103/PhysRevC.99.054904>
20. L.Y. Zhang, J.H. Chen, Z.W. Lin et al., Two-particle angular correlations in pp and p -Pb collisions at energies available at the cern large hadron collider from a multiphase transport model. *Phys. Rev. C* **98**, 034912 (2018). <https://doi.org/10.1103/PhysRevC.98.034912>
21. N. Armesto, C.A. Salgado, U.A. Wiedemann, Medium induced gluon radiation off massive quarks fills the dead cone. *Phys. Rev. D* **69**, 114003 (2004). <https://doi.org/10.1103/PhysRevD.69.114003>
22. M. Djordjevic, M. Gyulassy, Heavy quark radiative energy loss in QCD matter. *Nucl. Phys. A* **733**, 265–298 (2004). <https://doi.org/10.1016/j.nuclphysa.2003.12.020>
23. X. Zhu, N. Xu, P. Zhuang, Effect of partonic wind on charm quark correlations in high-energy nuclear collisions. *Phys. Rev. Lett.* **100**, 152301 (2008). <https://doi.org/10.1103/PhysRevLett.100.152301>
24. Z.W. Lin, C.M. Ko, B.A. Li et al., Multiphase transport model for relativistic heavy ion collisions. *Phys. Rev. C* **72**, 064901 (2005). <https://doi.org/10.1103/PhysRevC.72.064901>
25. T. Shao, J. Chen, C.M. Ko et al., Enhanced production of strange baryons in high-energy nuclear collisions from a multiphase transport model. *Phys. Rev. C* **102**, 014906 (2020). <https://doi.org/10.1103/PhysRevC.102.014906>
26. S. Zhang, Y.G. Ma, G.L. Ma et al., Collision system size scan of collective flows in relativistic heavy-ion collisions. *Phys. Letts. B* **804**, 135366 (2020). <https://doi.org/10.1016/j.physletb.2020.135366>
27. C. Zhang, L. Zheng, F. Liu et al., Update of a multiphase transport model with modern parton distribution functions and nuclear shadowing. *Phys. Rev. C* **99**, 064906 (2019). <https://doi.org/10.1103/PhysRevC.99.064906>
28. X.N. Wang, M. Gyulassy, Hijing: a monte carlo model for multiple jet production in pp, pA, and AA collisions. *Phys. Rev. D* **44**, 3501 (1991). <https://doi.org/10.1103/PhysRevD.44.3501>
29. M. Gyulassy, X. Wang, Hijing 1.0: a Monte Carlo program for parton and particle production in high-energy hadronic and nuclear collisions. *Comput. Phys. Commun.* **83**, 307–331 (1994). [https://doi.org/10.1016/0010-4655\(94\)90057-4](https://doi.org/10.1016/0010-4655(94)90057-4)
30. B. Zhang, Zpc 1.0.1: a parton cascade for ultrarelativistic heavy ion collisions. *Comput. Phys. Commun.* **109**, 193–206 (1998). [https://doi.org/10.1016/S0010-4655\(98\)00010-1](https://doi.org/10.1016/S0010-4655(98)00010-1)
31. T. Sjostrand, High-energy-physics event generation with pythia 5.7 and jetset 7.4. *Comput. Phys. Commun.* **82**, 74–89 (1994). [https://doi.org/10.1016/0010-4655\(94\)90132-5](https://doi.org/10.1016/0010-4655(94)90132-5)
32. B.A. Li, C.M. Ko, Formation of superdense hadronic matter in high energy heavy-ion collisions. *Phys. Rev. C* **52**, 2037–2063 (1995). <https://doi.org/10.1103/PhysRevC.52.2037>
33. D.W. Duke, J.F. Owens, Q^2 -dependent parametrizations of parton distribution functions. *Phys. Rev. D* **30**, 49–54 (1984). <https://doi.org/10.1103/PhysRevD.30.49>
34. L. Zheng, C. Zhang, S. Shi et al., Improvement of heavy flavor productions in a multi-phase transport model updated with modern npdfs. *Phys. Rev. C* **101**, 034905 (2020). <https://doi.org/10.1103/PhysRevC.101.034905>
35. T. Song, H. Berrehrah, D. Cabrera et al., Charm production in Pb + Pb collisions at energies available at the cern large hadron collider. *Phys. Rev. C* **93**, 034906 (2016). <https://doi.org/10.1103/PhysRevC.93.034906>